ELSEVIER

Contents lists available at ScienceDirect

Extreme Mechanics Letters

journal homepage: www.elsevier.com/locate/eml



Deformation and instability of three-dimensional graphene honeycombs under in-plane compression: Atomistic simulations



Luoxia Cao a, Feifei Fan a,b,*

- ^a Department of Mechanical Engineering, University of Nevada, Reno, Reno, NV 89557, USA
- ^b Nevada Institute for Sustainability, University of Nevada, Reno, Reno, NV 89557, USA

ARTICLE INFO

Article history: Received 21 February 2020 Received in revised form 24 June 2020 Accepted 24 June 2020 Available online 26 June 2020

Keywords: 3D graphene honeycomb Bending-type deformation Shear-type deformation Progressive buckling Localized shearing Molecular dynamics

ABSTRACT

While monolayer graphene is known strong and brittle, its three-dimensional (3D) scaleup to architected assemblies, such as graphene aerogels, leads to superior compressibility and resilience. 3D graphene assemblies feature nanoscale characteristic dimensions, and their constitutive mechanical behaviors arise from complex deformation modes. However, whether 3D graphene assemblies exhibit deformation mechanisms widely observed in conventional foams is unclear. Using molecular dynamics simulations, we explore the deformation and instability mechanisms in a 3D graphene honeycomb subjected to uniaxial in-plane compression. Our simulations capture the orientation-dependence of stress–strain response and deformation mode. Compression along the armchair direction causes progressive buckling and results in a structural transformation. In contrast, compression along the zigzag direction results in localized shearing. These findings demonstrate that deformation and instability mechanisms in 3D graphene honeycombs are very similar to those identified in hexagonal honeycombs at the macro-scale level, both experimentally and theoretically.

© 2020 Elsevier Ltd. All rights reserved.

1. Introduction

While monolayer graphene is strong and brittle [1–3], three-dimensional (3D) graphene assemblies exhibit superior compressibility and resilience [4–7]. These properties are important indicators of load-bearing and energy absorption capacities. The superior compressibility and resilience are attributed to bending and elastic buckling of graphene sheets in 3D graphene assemblies [5,8]. Geometry and architecture are then identified as leading parameters for deformation patterns. However, the ultra-low relative density of graphene assemblies and the high aspect ratio of graphene sheets with characteristic dimensions at the nanoscale pose challenges to conventional scaling laws [9]. To predict the compressive responses of bulk graphene assemblies thus needs an understanding of deformation and instability mechanisms in representative 3D graphene structures.

Graphene honeycombs, a 3D scaleup of graphene nanoribbons, are considered as a prototypical structure and demonstrated structurally stable [10–13]. One simple and representative graphene honeycomb structure is constituted by nanoribbons connected along zigzag or armchair edges through strong covalent bonds [11,13–15]. Conventional honeycombs, which are generally stiff and strong under out-of-plane compression, exhibit

E-mail address: ffan@unr.edu (F. Fan).

mechanism-rich behaviors when subjected to in-plane compression. The stress-strain curves of 3D honeycombs often exhibit distinct regimes, such as initial linear and nonlinear elastic, serrated plateau, and densification regimes [16-18]. The characteristics of these regimes result from a variety of deformation mechanisms. For instance, the local peaks in the serrated plateau can be associated with the initiation of collapse in a row of cells and the local valleys can be associated with the arrest of collapse as a result of contact between the cell walls [17]. In addition, the honeycomb's resilience and energy absorption capacity are closely related to the post-bifurcation regime and stable bifurcated configurations [19,20]. Inspired by previous experimental observations of deformation patterns in hexagonal metallic honeycombs and theoretical predictions of mechanical instabilities that take advantage of geometric regularity and periodicity, we ask a question: Does the continuum mechanics, e.g., pre-buckling and initial post-buckling responses of elastic periodic honeycombs, break down in 3D graphene honeycombs with characteristic dimensions at the nanoscale? Challenges to answer the question lie in the sensitivity of deformation mechanisms to nanoscale dimensions and possible nonlinearities. These challenges can be overcome by using molecular dynamics (MD) simulations.

In this work, we investigate the mechanical behavior of a 3D graphene honeycomb structure under in-plane compression using classical MD simulations. We report stress-strain responses and deformation mechanisms right before cell walls come into

^{*} Corresponding author at: Department of Mechanical Engineering, University of Nevada, Reno, Reno, NV 89557, USA.

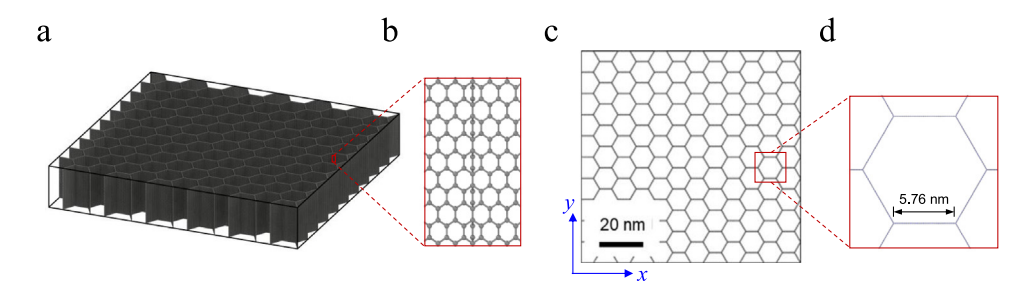


Fig. 1. Atomic structure of the 3D graphene honeycomb. (a) Perspective view. (b) Zoom-in view showing the detailed atomic configuration at cell junctions. (c) Projection view. (d) Zoom-in view showing a cell.

contact in the deformation history. Our simulations show that the honeycomb exhibits different deformation and instability mechanisms under in-plane compression along the armchair and the zigzag directions, and the onset of instability occurs primarily due to progressive nonlinear elastic buckling and the formation of a shear band. The findings highlight the decisive role of geometric nonlinearity in deformation modes and the consequent loss of strength and energy absorption capacity. This work poses an open-ended question regarding similarities in deformation modes between finitely strained periodic architectures and crystal lattices.

2. Modeling methods

We generated a 3D graphene honeycomb structure by connecting monolayer graphene sheets along their armchair edges (Fig. 1). Following the theoretical hypothesis of the atomic structure of cell junctions [13–15], we constructed 6-6-6 junctions that exhibit sp^3 -bonding to connect three neighboring graphene sheets. This atomic structure of junctions is predicted mechanically stable, and it is thus an energy-favorable configuration. Previous MD simulations of graphene honeycombs constituted by monolayer graphene were performed in systems either with a small cell size or with a relatively small number of cells [21-23]. These simulations are thus likely to suppress certain deformation mechanisms (e.g., shear bands and progressive buckling) and result in a low compressibility (densification strain). To well represent the high aspect ratio of building blocks in 3D graphene assemblies and to capture more possible deformation modes, our simulation system has a dimension of 105 nm \times 101 nm \times 17 nm with a cell size of 5.76 nm (Fig. 1). The system contains 1,407,120 atoms and consists of 12×10 cells.

We performed large-scale molecular dynamics simulations using the LAMMPS package [24]. We adopted the adaptive intermolecular reactive empirical bond order (AIREBO) potential [25] to describe the interatomic interactions. To avoid a non-physical post-hardening behavior under large strains, we set the cut-off distances in the AIREBO potential to 1.92 Å, as suggested by previous studies [3,26,27]. To eliminate the boundary effect, we imposed the periodic boundary condition in all three directions. Prior to applying any loading, we performed stress relaxation in the isothermal isobaric (NPT) ensemble at a temperature of 300K for 500 ps. We then performed in-plane uniaxial compression tests by rescaling the dimension of the simulation box along the loading direction with a constant strain rate of 10^7 s⁻¹ at 300K. This strain rate is sufficiently slow for investigating the mechanical behavior of our system, whose base material is elastic and brittle [28,29]. In the two non-loading directions, the corresponding box dimensions were free to change. The time step was 1fs in all simulations. The coordinate system for the compression tests is specified in Fig. 1. x and y axes are along the armchair and zigzag directions, respectively, and z axis is along the out-of-plane direction.

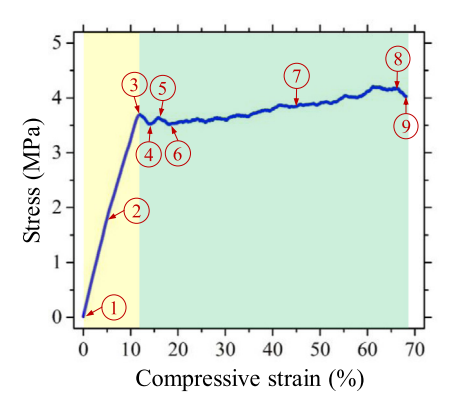


Fig. 2. Effective engineering stress–strain curve of the graphene honeycomb subjected to uniaxial compression in x direction.

3. Results and discussion

The compressive behaviors of hexagonal, metallic honeycombs under in-plane uniaxial compression usually exhibit three regimes: (1) stable and nearly uniform deformation and a resulting relatively high stiffness. (2) coexistence of collapsed and uncollapsed deformation and a resulting essentially zero stiffness, and (3) densification with relatively uniform and stable collapsed deformation and a much stiffer response [16,30]. In this work, we examine the stress-strain curves and the deformation mechanisms up to the onset of densification, where post contact of cell walls and extensive irreversibility take place. One reason to only examine the behavior before densification is that beyond the densification strain the energy absorption efficiency (i.e., specific energy absorbed up to a given nominal strain normalized by the corresponding stress value) may drop rapidly [17]. Another reason is that post contact of cell walls, which is usually accompanied by sliding and irreversibility, challenges the interatomic potential and increases the complexities of the constitutive behavior of the honeycomb structure [31].

Fig. 2 shows the effective engineering stress–strain curve of the graphene honeycomb under uniaxial compression along x direction (*i.e.*, the load normalized by the undeformed effective cross-sectional area versus the applied displacement normalized by the undeformed x dimension of the system). The honeycomb undergoes compression up to an engineering strain of 69%, after which post contact of cell walls causes unrealistic bond changes. The stress–strain curve exhibits a stable and nearly linear regime followed by a serrated plateau. In the initial linear regime, the effective stress monotonically and linearly increases with the effective strain. This monotonicity indicates that the honeycomb undergoes relatively uniform and stable cell deformation. In the plateau regime, which follows the load at the onset of instability,

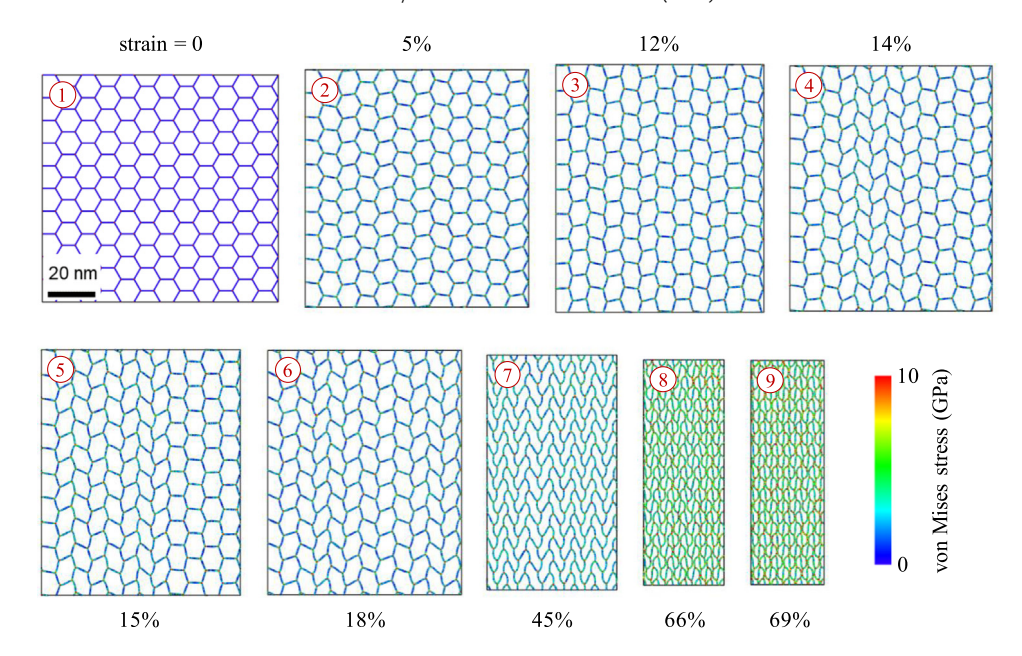


Fig. 3. Projection views (along the out-of-plane direction) of the deformed configurations at different deformation stages in Fig. 2. Atoms are colored by the von Mises stress, which is calculated from the Virial stress of each atom.

the effective stress undulates with a small amplitude about a relatively constant level. The stress plateau and undulations suggest a progressive process of localized deformation.

Fig. 3 provides a sequence of morphological configurations (viewed in the z direction) of the honeycomb loaded in x direction. During compression up to 12%, the inclined cell walls deform primarily through bending around junctions, and the non-inclined walls rotate to accommodate compatibility (configurations (2) - (3)). After the first peak stress, the linear regime is terminated by buckling of cell walls, and the effective stress starts to decrease until a compressive strain of 14%. As shown in configuration (4), the deformation starts to localize in a row-by-row manner. To accommodate the applied strain in x direction from 12% to 14%, certain rows of cells deform significantly, while the rest rows remain relatively unaffected. The propagation of such row-by-row deformation, as also shown in configurations (5) and (6), features the coexistence of newly deformed rows and rows with negligible new deformation. In the following loading history, each row of cells repeats this deformation process and the deformation eventually spreads throughout the entire honeycomb structure. The stress-strain curve becomes smoother because the progressive row-by-row deformation continues at smaller displacement increments (as shown in configuration ⑦). The overall positive slope of the stress-strain curve at this stage indicates that further deformation requires an increase in load. The configurations closely follow a post-bifurcated anti-rolls mode associated with breaking of symmetry predicted based on a homogenization theory of finite deformation [20]. Finally, right before post contact of cell walls, most cell walls develop a state of high stress (configurations (8) and (9)). The transverse deformation, which associates with the v dimension of the simulation system, increases in the linear regime and then decreases in the plateau regime. During the entire course of deformation in the present problem, breaking and reforming of atomic bonds are not observed. Since single layer graphene is linear elastic and contact is not involved, we rule out the effect of material nonlinearity and the nonlinearity due to contact. We then attribute the mechanical instability and the repetitively progressive buckling primarily to geometric nonlinearity. We note that the resulting structural transformation induced by this progressive bucklingtype deformation is analogous to a phase transformation in single crystals.

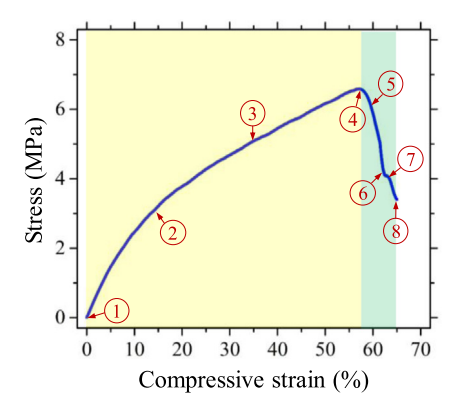


Fig. 4. Effective engineering stress-strain curve of the graphene honeycomb subjected to uniaxial compression in *y* direction.

Unlike the response to compression in x direction, the response to compression in y direction cannot be divided into a linear regime and a plateau regime. Fig. 4 shows the effective engineering stress-strain curve of the graphene honeycomb under uniaxial compression along y direction (i.e., the load normalized by the undeformed effective cross-sectional area versus the applied displacement normalized by the undeformed y dimension of the system). The honeycomb undergoes compression up to an engineering strain of 65%, after which an avalanche of unrealistic bond changes takes place. We divide the stress-strain curve into two regimes: the first has a positive slope and the second has a negative slope. In the first regime, the effective stress monotonically increases with the effective strain, but the slope decreases. The response becomes progressively nonlinear and exhibits a gradual reduction in stiffness. This nonlinear and monotonically increasing response suggests that the honeycomb deforms essentially in a uniform fashion. The second regime starts at the peak stress, which corresponds to the onset of instability. The effective stress starts to drop, and this sudden drop indicates that the structure develops a catastrophic instability.

Fig. 5 provides a sequence of morphological configurations (viewed in the z direction) of the honeycomb loaded in y direction. During compression up to 57% (configurations (1) – (4)),

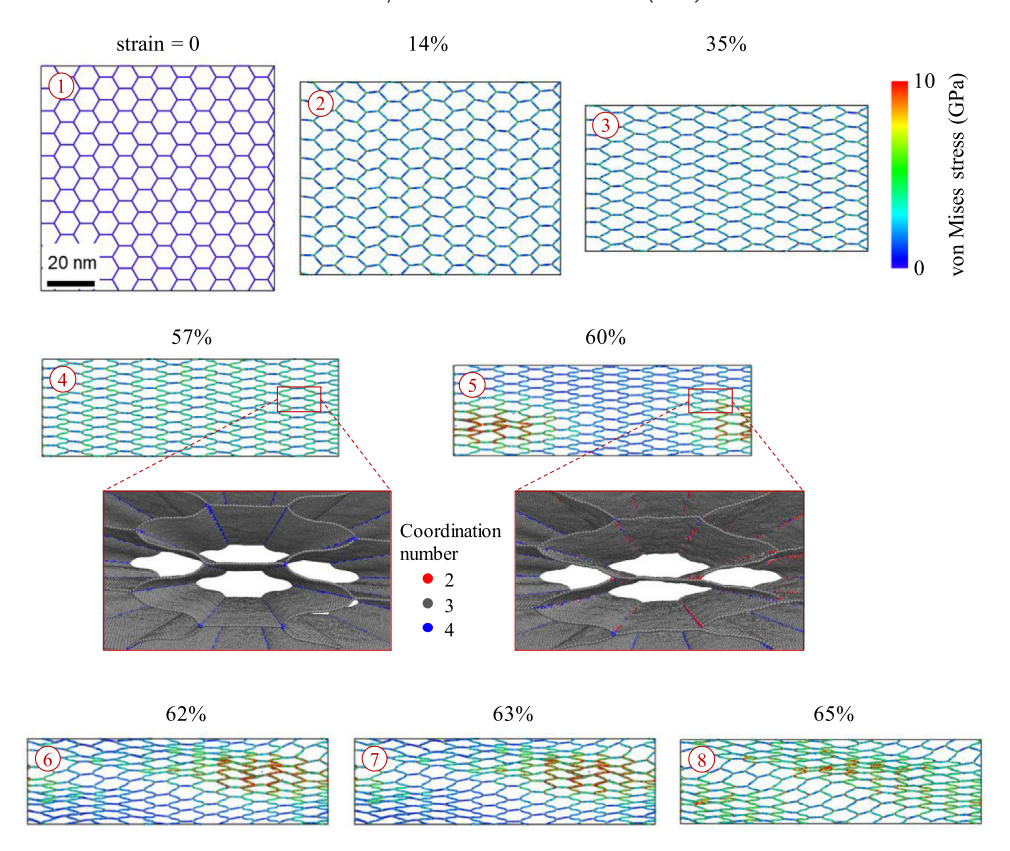


Fig. 5. Projection views (along the out-of-plane direction) of the deformed configurations at different deformation stages in Fig. 4. Atoms are colored by the von Mises stress, which is calculated from the Virial stress of each atom.

the inclined cell walls deform through bending around junctions. The non-inclined walls are under stretch without large rotation and limit the transverse deformation. Material points experience monotonic loading due to the bending and stretching of the cell walls. The honeycomb deforms primarily symmetrically about the axis of loading and remains stable up to the onset of instability (configuration (4)). Beyond this point, the cell deformation ceases to be uniform and instead starts to localize in a relatively small region of the honeycomb (configuration (5)). Covalent bonds at cell junctions start to break (inset of Fig. 5), which contrasts with the suppression of bond breaking and reforming under compression in x direction. Under further deformation, the initial localized cell deformation propagates and is transmitted to neighboring cells (configurations 6 - 8), developing a shear band at an angle to the loading axis. Cells adjacent to this shear band recover some of their original shape by partially releasing the deformation. The load required to propagate such a shear band is substantially lower than that required to initiate it. This nonsymmetric (sheartype) deformation results in a negative slope of the effective stress-strain curve. The presence of the negative slope suggests that this localized shear-type deformation is energetically preferable to uniform bending deformation. Accompanied by the shear band, the honeycomb develops a localized band of high stress. During the compression, the transform deformation of the honeycomb increases until the onset of the instability; however, the subsequent shearing does not change the overall transverse deformation obviously. We note that such an instability in the form of a shear band and the associated stress drop are analogous to a dislocation slip and the associated stress drop in single crystals.

To examine the influence of different deformation mechanisms on energy absorption, we characterize two parameters. One is specific energy absorption, which is the total energy absorbed divided by the total mass and determined by the area under the stress–strain curve. The other is energy absorption efficiency,

which is the specific energy absorption normalized by the corresponding stress. Fig. 6 compares the energy absorption capacities of the graphene honeycomb under uniaxial compression in x and y directions. Fig. 6a shows that for a compressive strain higher than 30%, the specific energy absorption under compression in y direction is higher than that in x direction. This comparison suggests that the bending-type deformation results in a higher energy absorption capacity than the progressive buckling-type deformation. Fig. 6b shows that for a compressive strain higher than 15%, but before the onset of shear-type deformation, the energy absorption efficiency under compression in x direction is higher than that in y direction, although the subsequent shear-type deformation increases the energy absorption efficiency due to the sudden stress drop.

The simulated instability mechanisms in the graphene honeycomb are similar to buckling and failure modes observed in hexagonal, metallic honeycombs at the macro-scale level, both experimentally [16,18,32] and theoretically [20,33-35]. The buckling mode obtained in our MD simulation (configuration (7) in Fig. 3) agrees with the buckling pattern predicted based on a homogenization theory [16,20,34]. The simulated progressive buckling behavior (configurations 3) - 7) in Fig. 3) and the corresponding stress-strain curve (Fig. 2) are similar to those reported in experiments and finite element simulations of conventional honeycombs subjected to uniaxial compression in the armchair direction [16,18,32,33,35]. On the other hand, the shear band mode in our simulation (configurations (6) – (8) in Fig. 5) is similar to the failure mode observed in conventional honeycombs subjected to uniaxial compression in the zigzag direction [18,33,35]. We thus suggest that theoretical predictions and experimental results of instability mechanisms in conventional honeycomb structures are applicable to graphene honeycombs.

As a final note, we comment on the possible influence of cell size on deformation and instability mechanisms. The pioneering

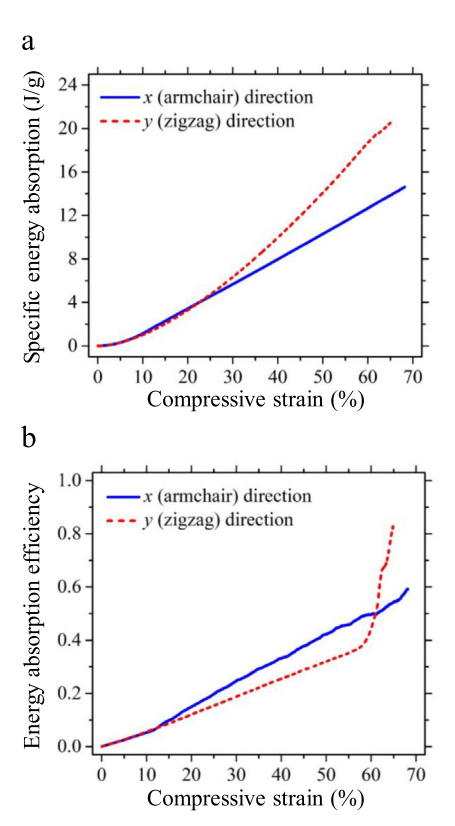


Fig. 6. Comparison of energy absorption capacities under compression in x and y directions. (a) Specific energy absorption–strain curves. (b) Energy absorption efficiency–strain curves.

investigation by Papka and Kyriakides on hexagonal, aluminum honeycombs has shown that cell geometric parameters and the relative density quantitatively affect the effective stress–strain response to uniaxial in-plane crushing [16]. It is thus reasonable to speculate that for graphene honeycombs the cell size can influence the initial slope of the effective stress–strain curve, the stress at the onset of instability (initiation stress), and the average stress of the plateau (propagation stress). Before cell walls come into contact, the major source of nonlinearities in such graphene honeycombs is geometry, and we expect that cell size would not change the qualitative nature of the deformation and instability mechanisms. However, it is conceivable that an extremely large cell size might induce cell wall contact before densification (e.g., in the progressive buckling stage) and pronounced out-of-plane deformations (e.g., ripples) in individual graphene sheets.

4. Conclusions

In conclusion, we have investigated the in-plane uniaxial compressive responses of a honeycomb structure constituted by monolayer graphene using MD simulations. Under compression in the armchair direction, the honeycomb experiences an initial linear response, followed by a serrated stress plateau due to progressive buckling-type deformation. In contrast, under compression along the zigzag direction, the honeycomb exhibits a nonlinear response associated with symmetric bending-type deformation and a following stress drop due to a shear-type instability. The results highlight the decisive role of geometric nonlinearity in deformation mechanisms and resulting load bearing and energy absorption capacities. The results also demonstrate that graphene honeycombs exhibit similar deformation and instability mechanisms to conventional hexagonal honeycombs at the macro-scale

level. Finally, we note that the instabilities in graphene honeycombs can be analogous to a phase transformation and a dislocation slip in single crystals.

Declaration of competing interest

The authors declare that they have no known competing financial interests or personal relationships that could have appeared to influence the work reported in this paper.

Acknowledgment

F. Fan acknowledges the support by the U.S. National Science Foundation (NSF) under the grant CMMI-1923033.

References

- C. Lee, X. Wei, J.W. Kysar, J. Hone, Measurement of the elastic properties and intrinsic strength of monolayer graphene, Science 321 (2008) 385.
- [2] G.-H. Lee, R.C. Cooper, S.J. An, S. Lee, A. van der Zande, N. Petrone, A.G. Hammerberg, C. Lee, B. Crawford, W. Oliver, J.W. Kysar, J. Hone, High-strength chemical-vapor-deposited graphene and grain boundaries, Science 340 (2013) 1073.
- [3] P. Zhang, L. Ma, F. Fan, Z. Zeng, C. Peng, P.E. Loya, Z. Liu, Y. Gong, J. Zhang, X. Zhang, P.M. Ajayan, T. Zhu, J. Lou, Fracture toughness of graphene, Nature Commun. 5 (2014) 3782.
- [4] Q. Zhang, X. Xu, H. Li, G. Xiong, H. Hu, T.S. Fisher, Mechanically robust honeycomb graphene aerogel multifunctional polymer composites, Carbon 93 (2015) 659–670.
- [5] M. Yang, N. Zhao, Y. Cui, W. Gao, Q. Zhao, C. Gao, H. Bai, T. Xie, Biomimetic architectured graphene aerogel with exceptional strength and resilience, ACS Nano 11 (2017) 6817–6824.
- [6] Z. Han, Z. Tang, S. Shen, B. Zhao, G. Zheng, J. Yang, Strengthening of graphene aerogels with tunable density and high adsorption capacity towards Pb2+, Sci. Rep. 4 (2014) 5025.
- [7] R.M. Hensleigh, H. Cui, J.S. Oakdale, J.C. Ye, P.G. Campbell, E.B. Duoss, C.M. Spadaccini, X. Zheng, M.A. Worsley, Additive manufacturing of complex micro-architected graphene aerogels, Mater. Horiz. 5 (2018) 1035–1041.
- [8] Q. Zhang, X. Xu, D. Lin, W. Chen, G. Xiong, Y. Yu, T.S. Fisher, H. Li, Hy-perbolically patterned 3D graphene metamaterial with negative Poisson's ratio and superelasticity, Adv. Mater. 28 (2016) 2229–2237.
- [9] Z. Qin, G.S. Jung, M.J. Kang, M.J. Buehler, The mechanics and design of a lightweight three-dimensional graphene assembly, Sci. Adv. 3 (2017) e1601536.
- [10] H.R. Karfunkel, T. Dressler, New hypothetical carbon allotropes of remarkable stability estimated by MNDO solid-state SCF computations, J. Am. Chem. Soc. 114 (1992) 2285–2288.
- [11] N.V. Krainyukova, E.N. Zubarev, Carbon honeycomb high capacity storage for gaseous and liquid species, Phys. Rev. Lett. 116 (2016) 055501.
- [12] Y. Gao, Y. Chen, C. Zhong, Z. Zhang, Y. Xie, S. Zhang, Electron and phonon properties and gas storage in carbon honeycombs, Nanoscale 8 (2016) 12863–12868.
- [13] Z. Pang, X. Gu, Y. Wei, R. Yang, M.S. Dresselhaus, Bottom-up design of three-dimensional carbon-honeycomb with superb specific strength and high thermal conductivity, Nano Lett. 17 (2017) 179–185.
- [14] N. Park, J. Ihm, Electronic structure and mechanical stability of the graphitic honeycomb lattice, Phys. Rev. B 62 (2000) 7614–7618.
- [15] A. Kuc, G. Seifert, Hexagon-preserving carbon foams: Properties of hypothetical carbon allotropes, Phys. Rev. B 74 (2006) 214104.
- [16] S.D. Papka, S. Kyriakides, In-plane compressive response and crushing of honeycomb, J. Mech. Phys. Solids 42 (1994) 1499–1532.
- [17] T. Jin, Z. Zhou, Z. Wang, G. Wu, X. Shu, Experimental study on the effects of specimen in-plane size on the mechanical behavior of aluminum hexagonal honeycombs, Mater. Sci. Eng. A 635 (2015) 23–35.
- [18] M. Xu, Z. Xu, Z. Zhang, H. Lei, Y. Bai, D. Fang, Mechanical properties and energy absorption capability of AuxHex structure under in-plane compression: Theoretical and experimental studies, Int. J. Mech. Sci. 159 (2019) 43–57.
- [19] C. Combescure, P. Henry, R.S. Elliott, Post-bifurcation and stability of a finitely strained hexagonal honeycomb subjected to equi-biaxial in-plane loading, Int. J. Solids Struct. 88–89 (2016) 296–318.
- [20] N. Ohno, D. Okumura, H. Noguchi, Microscopic symmetric bifurcation condition of cellular solids based on a homogenization theory of finite deformation, J. Mech. Phys. Solids 50 (2002) 1125–1153.
- [21] F. Meng, C. Chen, D. Hu, J. Song, Deformation behaviors of three-dimensional graphene honeycombs under out-of-plane compression: Atomistic simulations and predictive modeling, J. Mech. Phys. Solids 109 (2017) 241–251.

- [22] H. Wang, Q. Cao, Q. Peng, S. Liu, Atomistic study of mechanical behaviors of carbon honeycombs, Nanomaterials (Basel, Switzerland) 9 (2019) 109.
- [23] Z. Zhang, A. Kutana, Y. Yang, N.V. Krainyukova, E.S. Penev, B.I. Yakobson, Nanomechanics of carbon honeycomb cellular structures, Carbon 113 (2017) 26–32.
- [24] S. Plimpton, Fast parallel algorithms for short-range molecular dynamics, J. Comput. Phys. 117 (1995) 1–19.
- [25] S.J. Stuart, A.B. Tutein, J.A. Harrison, A reactive potential for hydrocarbons with intermolecular interactions, J. Chem. Phys. 112 (2000) 6472–6486.
- [26] H. Zhao, K. Min, N.R. Aluru, Size and chirality dependent elastic properties of graphene nanoribbons under uniaxial tension, Nano Lett. 9 (2009) 3012–3015.
- [27] Y. Wei, J. Wu, H. Yin, X. Shi, R. Yang, M. Dresselhaus, The nature of strength enhancement and weakening by pentagon-heptagon defects in graphene, Nature Mater. 11 (2012) 759–763.
- [28] F. Liu, R. Zou, N. Hu, H. Ning, C. Yan, Y. Liu, L. Wu, F. Mo, Understanding the mechanical properties and deformation behavior of 3-D graphene-carbon nanotube structures, Mater. Des. 160 (2018) 377–383.

- [29] H. Zhao, N.R. Aluru, Temperature and strain-rate dependent fracture strength of graphene, J. Appl. Phys. 108 (2010) 064321.
- [30] A.-J. Wang, D.L. McDowell, In-plane stiffness and yield strength of periodic metal honeycombs, J. Eng. Mater. Technol. 126 (2004) 137–156.
- [31] Z. Shen, H. Ye, C. Zhou, M. Kröger, Y. Li, Size of graphene sheets determines the structural and mechanical properties of 3D graphene foams, Nanotechnology 29 (2018) 104001.
- [32] S.D. Papka, S. Kyriakides, Biaxial crushing of honeycombs: —Part 1: Experiments, Int. J. Solids Struct. 36 (1999) 4367–4396.
- [33] S.D. Papka, S. Kyriakides, In-plane biaxial crushing of honeycombs—: Part II: Analysis, Int. J. Solids Struct. 36 (1999) 4397–4423.
- [34] I. Saiki, K. Terada, K. Ikeda, M. Hori, Appropriate number of unit cells in a representative volume element for micro-structural bifurcation encountered in a multi-scale modeling, Comput. Methods Appl. Mech. Engrg. 191 (2002) 2561–2585.
- [35] N. Triantafyllidis, M.W. Schraad, Onset of failure in aluminum honeycombs under general in-plane loading, J. Mech. Phys. Solids 46 (1998) 1089–1124.